Journal of The Electrochemical Society, **159** (2) A98-A103 (2012)
0013-4651/2012/159(2)/A98/6/$28.00 © The Electrochemical Society

The Effect of Insertion Species on Nanostructured Open Framework Hexacyanoferrate Battery Electrodes

Colin D. Wessells,[a] Sandeep V. Peddada,[a] Matthew T. McDowell,[a] Robert A. Huggins,[a,*] and Yi Cui[a,b,*,z]

[a]*Department of Materials Science and Engineering and* [b]*Stanford Institute for Materials & Energy Science, SLAC National Accelerator Laboratory, Stanford University, Stanford, California 94305, USA*

Recent battery research has focused on the high power and energy density needed for portable electronics and vehicles, but the requirements for grid-scale energy storage are different, with emphasis on low cost, long cycle life, and safety.[1,2] Open framework materials with the Prussian Blue crystal structure offer the high power capability, ultra-long cycle life, and scalable, low cost synthesis and operation that are necessary for storage systems to integrate transient energy sources, such as wind and solar, with the electrical grid. We have demonstrated that two open framework materials, copper hexacyanoferrate and nickel hexacyanoferrate, can reversibly intercalate lithium, sodium, potassium, and ammonium ions at high rates. These materials can achieve capacities of up to 60 mAh/g. The porous, nanoparticulate morphology of these materials, synthesized by the use of simple and inexpensive methods, results in remarkable rate capabilities: e.g. copper hexacyanoferrate retains 84% of its maximum capacity during potassium cycling at a very high (41.7C) rate, while nickel hexacyanoferrate retains 66% of its maximum capacity while cycling either sodium or potassium at this same rate. These materials show excellent stability during the cycling of sodium and potassium, with minimal capacity loss after 500 cycles.
 [DOI: 10.1149/2.060202jes]

Manuscript submitted September 6, 2011; revised manuscript received November 7, 2011. Published December 19, 2011.

Despite a rapidly growing need for large-scale energy storage capacity integrated with the electrical power grid, most recent research and commercial development of batteries has focused on materials systems primarily suitable for use in portable electronics and vehicles, for which the amount of energy storage per unit weight or volume is the critical issue.[1–3] Energy storage capacity is urgently needed to handle the management of short-term transients and the related frequency regulation problems on the electrical grid. This has become extremely costly,[4] and in coming years, the increasing use of intermittent power sources, such as wind and solar, will greatly increase the need for the development of suitable large scale storage capacity for such purposes.[5]

Current grid-scale energy storage systems using compressed air and pumped hydropower suffer from low energy efficiency, and are limited to select locations.[1,6] While flywheel systems can be efficient and accommodate high power input and output, they cannot provide large amounts of energy storage. Existing battery technologies cannot provide sufficient cycle life, high input/output power, and round trip energy efficiency at a low enough cost to allow their rapid deployment to support the grid.[1,2] Inexpensive lead-acid batteries operate over only a limited depth of discharge, while still suffering from poor cycle life and energy efficiency. Redox flow batteries and sodium/nickel chloride (Zebra) cells cannot operate at high enough power levels. Other alternatives, such as sodium/sulfur, nickel/metal hydride, and lithium-ion batteries offer better performance, but cost too much to be the primary energy storage medium for use with the grid. Recent results on aqueous lithium-ion and sodium-ion systems have shown promising results, but this technology has yet to be fully developed.[7–10] Therefore, new materials systems are necessary for the inexpensive, efficient, durable, high-power batteries needed for use in connection with the grid.

One alternative is to use metal-organic framework (MOF) materials, some of which are known to reversibly intercalate molecular species such as hydrogen, and various ions.[11,12] Recently, MOFs relying on the Fe^{+3}/Fe^{+2} couple were demonstrated for use as lithium ion battery cathodes in an organic electrolyte.[13] This paper reports results using two open electrode materials, copper hexacyanoferrate (CuHCF), and nickel hexacyanoferrate (NiHCF), which both have the Prussian Blue crystal structure, and readily intercalate a variety of ions, including Li^+, Na^+, K^+ and NH_4^+, when operated in aqueous electrolytes.

Prussian Blue, the oldest and most studied mixed-valence material of this type, has the archetypal hexacyanometalate framework structure.[14] Materials with the Prussian Blue structure may be described in terms of the general formula $A_xPR(CN)_6$.[15–17] Nitrogen-coordinated transition metal cations (P) and hexacyanometalate complexes ($R(CN)_6$) form a face-centered cubic open framework containing large interstitial A sites, which may be partially or fully occupied by a number of different hydrated ions in this structure (Fig. 1a). The ionic occupancy of these A sites may vary between 0 and 2, with corresponding valence changes in one or both of the P and R species.[18]

The electrochemical activity of Prussian Blue, which also exhibits electrochromism, was first demonstrated by Neff.[19] Subsequently, other hexacyanoferrates containing alkali ions were also found to show electrochemical activity.[18,20–23] The robust framework structure of Prussian Blue and its analogs has been shown to allow thin film electrochromic devices to operate for 10^5 to 10^7 cycles at high cycling rates.[24,25] Thin films of Prussian Blue and its analogs were also earlier investigated for use in batteries,[26–30] but the 300 nm films typically employed had such low mass loading ($\mu g/cm^2$) that they were not practically useful.[25]

In contrast to the earlier work on Prussian Blue analog thin films, the behavior of bulk CuHCF and NiHCF electrodes was recently examined,[31,32] and more detailed results are described here. They were about 100 μm thick, with mass loadings of 5–10 mg/cm^2, similar to those used in current lithium-ion batteries. It was found that these relatively inexpensive materials possess remarkable electrochemical performance, operate in safe, inexpensive aqueous electrolytes, and may be synthesized using bulk processes at modest temperatures. Hence, they are especially attractive for use in large-scale stationary batteries to provide storage capacity for use with the electrical power grid.

Although potassium has been the most common intercalant in electrochromic devices using Prussian Blue and its analogs, there has been some previous work on thin films of Prussian Blue, NiHCF, and other materials with this structure that showed electrochemical activity in the presence of a variety of other aqueous cations.[20–23,30,33] One of the objectives of the present work was to examine the effect of the identity of the inserted species on the electrochemical properties of bulk CuHCF and NiHCF. Thus, the electrochemical behavior of these two Prussian Blue analog materials in

* Electrochemical Society Active Member.
z E-mail: yicui@stanford.edu

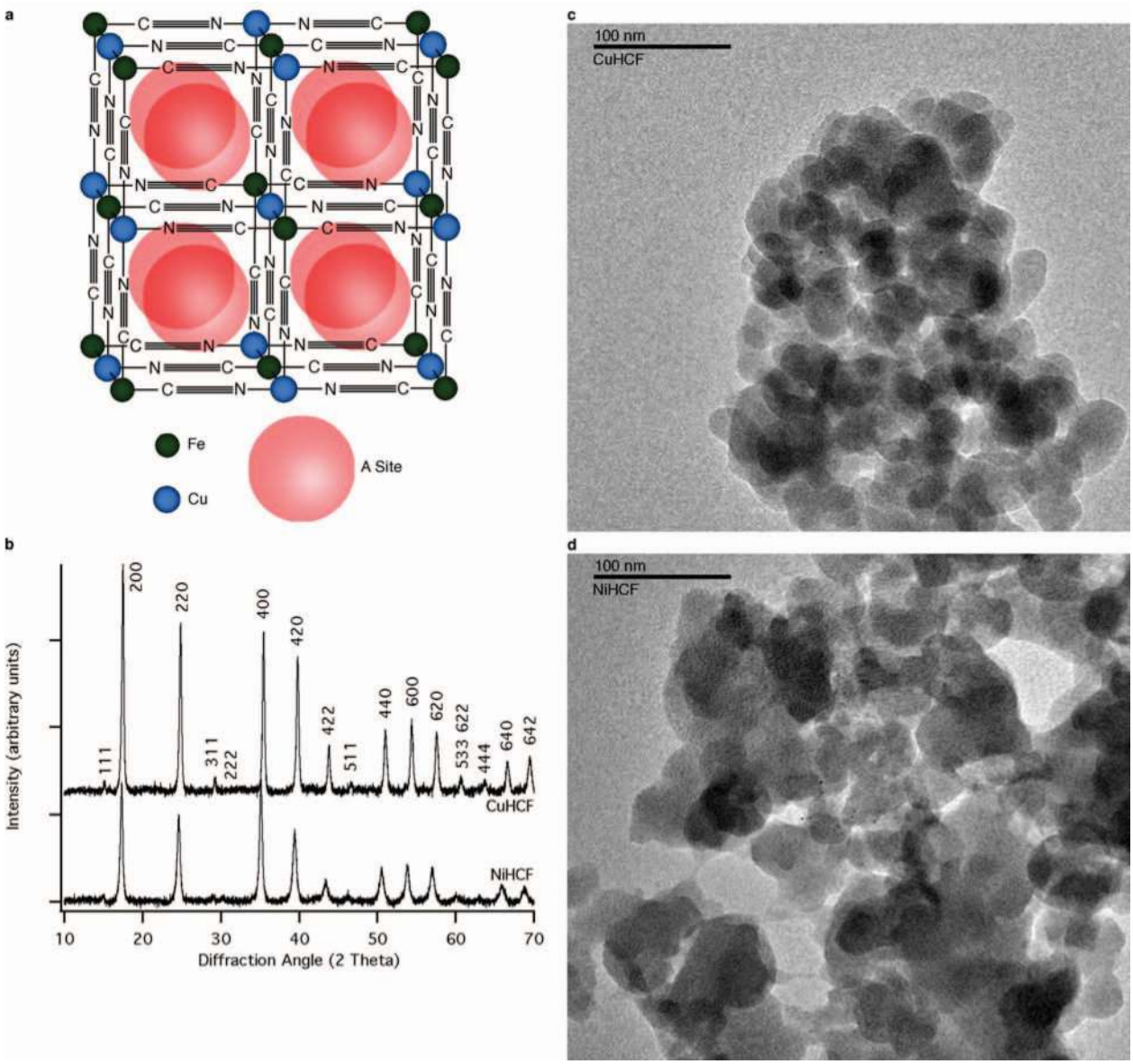

Figure 1. (a) The unit cell of the Prussian Blue crystal structure has an open framework of octagonal hexacyanometalate groups such as $Fe(CN)_6$ linked by nitrogen-coordinated transition metal cations such as Ni^{+2} and Cu^{+2}. Each of the eight subcells within the unit cell contains a large, open "A site", which may contain zeolitic water or hydrated ions (omitted for clarity). Changes in the occupancy of the A sites by ions occurs during oxidation changes of transition metal ions in the framework. (b) The fully-indexed x-ray diffraction spectra of the as-synthesized NiHCF and CuHCF shows that both materials are phase pure, with the FCC Prussian Blue crystal structure. (c) and (d) Transmission electron microscopy of CuHCF and NiHCF, respectively, show porous agglomerations of 20–50 nm grains.

aqueous electrolytes containing Li^+, Na^+, K^+, and NH_4^+ ions was investigated.

Experimental

Both CuHCF and NiHCF were synthesized as nanopowders. This was done using a simple co-precipitation method. Simultaneous, dropwise addition of 40 mM copper or nickel nitrate, and 20 mM potassium ferricyanide into deionized water produced controlled precipitation of uniform fine particles of both CuHCF or NiHCF. The synthesis of CuHCF was done at room temperature, while the synthesis of NiHCF was performed at 70°C. These solid products were filtered, washed with water, and dried in vacuum at room temperature. Up to 3 g of product was typically produced during each synthesis, and this method can be readily scaled to produce much larger quantities of either CuHCF or NiHCF. Slurries containing the as-synthesized hexacyanoferrates, amorphous carbon (Timcal SuperP Li), polyvinylidene difluoride (Kynar HSV 900), and graphite (Timcal KS6) in a ratio of 80:9:9:2 were prepared in 1-methyl-2-pyrrolidinone. These slurries were deposited on carbon cloth, and dried in vacuum at no more than 80°C.

Three-electrode flooded cells containing a CuHCF or NiHCF working electrode, a Ag/AgCl reference electrode, and a large, partially charged CuHCF or NiHCF counter electrode were used to study the electrochemical behavior of CuHCF and NiHCF in various aqueous electrolytes. The electrolytes used were aqueous 1 M $LiNO_3$, 1 M $NaNO_3$, 1 M KNO_3, and 0.5 M $(NH_4)_2SO_4$. The pH of all electrolytes was lowered to 2 by the addition of nitric or sulfuric acid. The counter electrodes functioned as reversible ion sinks, analogous to the large mass of metallic lithium typically used for lithium-ion half-cells. After synthesis, both CuHCF and NiHCF initially contained some potassium. To avoid contamination of the

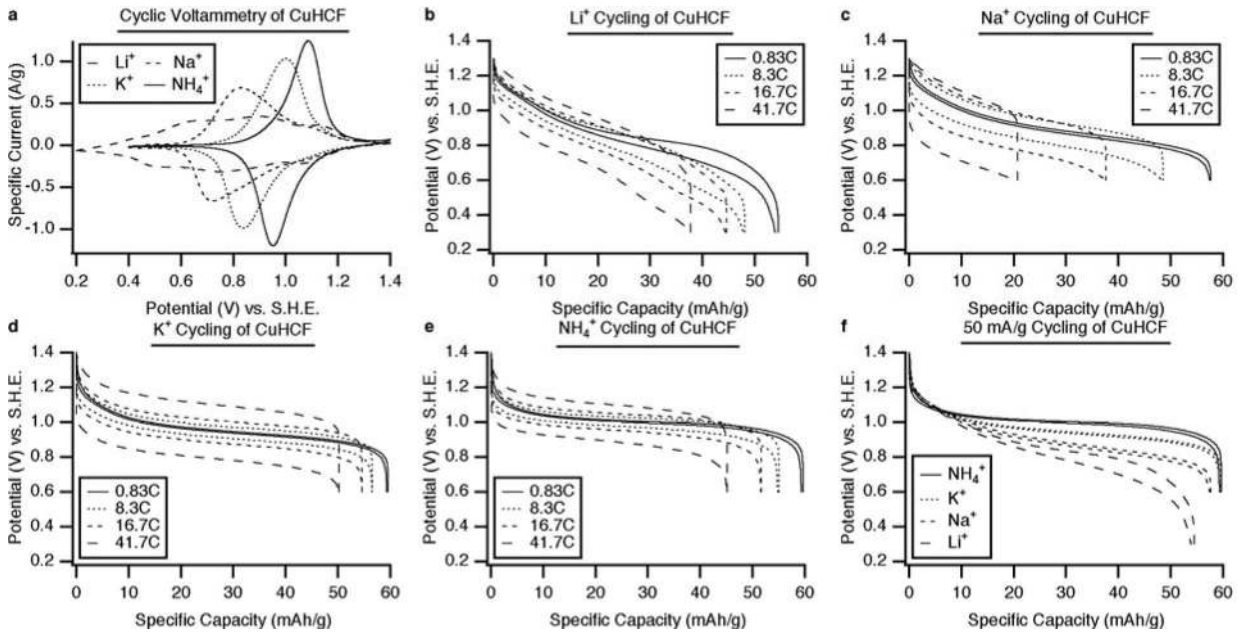

Figure 2. Electrochemical performance of CuHCF. (a) Cyclic voltammetry of CuHCF with Li^+, Na^+, K^+ and NH_4^+ ions, and (b) through (e): The potential profiles of CuHCF during galvanostatic cycling of Li^+, Na^+, K^+, and NH_4^+, respectively, at several current densities. (f) The potential profiles of CuHCF during galvanostatic cycling of Li^+, Na^+, K^+, and NH_4^+, at 50 mA/g (0.83C).

lithium, sodium, and ammonium-containing electrolytes by potassium de-intercalated from the counter electrodes, the counter electrodes were pretreated. First, as much potassium as possible was removed from them by fixing their potentials at 1.1 V vs. S.H.E. until the current decayed to zero. After washing with water, they were then partially discharged in fresh electrolyte by fixing their potentials at the half-charge potentials of CuHCF and NiHCF in each electrolyte. Each working and counter electrode was used in only one type of electrolyte.

Results and Discussion

CuHCF and NiHCF were characterized by inductively coupled plasma mass spectrometry (ICP-MS), powder x-ray diffraction and scanning electron microscopy. Elemental analysis by ICP-MS found that CuHCF had a composition of $K_{0.9}Cu_{1.3}Fe(CN)_6$, while the stoichiometry of NiHCF was $K_{0.6}Ni_{1.2}Fe(CN)_6$. Both materials were found to be phase-pure, with the face-centered cubic Prussian Blue crystal structure (Fig. 1b).[16,17] The lattice parameter of the as-synthesized CuHCF powder was 10.16 Å, while the lattice parameter of the NiHCF powder was 10.22 Å. Transmission electron microscopy showed that both materials consisted of large, porous agglomerations of 20–50 nm nanoparticles (Fig. 1c–1d). Electron diffraction spectra for these materials could not be observed due to the instability of their MOF frameworks during exposure to the electron beam. The small particle size and porous nature of the agglomerates is advantageous for use in battery electrodes, as the high surface-to-volume ratio of nanoparticles allows inserted ions to rapidly diffuse throughout the material. Past studies of similar Prussian Blue analogs have found specific surface areas of up to 870 m^2/g using BET analysis.[34]

To characterize the electrochemical behavior of CuHCF and NiHCF, cyclic voltammetry and galvanostatic cycling of these materials were performed in aqueous electrolytes containing Li^+, Na^+, K^+, or NH_4^+ ions. Impedance spectroscopy experiments were undertaken using an experimental setup similar to that employed during galvanostatic cycling. However, the high mass loading, inhomogeneity, and non-planar geometry of the electrodes made quantitative interpretation difficult. As a result, they are not included here. The charge transfer resistance of Prussian Blue analog thin films was typically found to be about 1 Ω/cm^2.[23]

Cyclic voltammetry scans at 1 mV/s were performed on both CuHCF and NiHCF with all four insertable cations over wide potential ranges (Fig. 2a and 3a). CuHCF has single, sharp reactions with K^+, and NH_4^+, centered at approximately 0.93 V and 1.02 V vs. S.H.E., respectively. The behavior of CuHCF with Li^+ and Na^+ during cyclic voltammetry is more complex as three broad reactions are observed between 0.4 and 1.2 V during Li^+ cycling, and the strong reaction with Na^+ at 0.77 V is followed by a shoulder near 1.0 V. Cyclic voltammetry of NiHCF showed sharp reactions with Na^+ and K^+ at 0.59 and 0.69 V, respectively, a slightly broader reaction with NH_4^+ at 0.75 V, and finally, broad reaction with Li^+ centered at 0.37 V, with an upper shoulder near 0.7 V. While the cyclic voltammetry measurements provided insight about the reaction potentials of CuHCF and NiHCF, galvanostatic cycling is attractive because it simulates the constant current conditions under which batteries often operate. The cycling was performed over a wide range of current densities, between ±10 and ±2500 mA/g of active material.

Specific capacities of 60 mAh/g were measured for both CuHCF and NiHCF during slow cycling in electrolytes containing Li^+, Na^+, K^+, or NH_4^+. For comparision, common lithium-ion battery cathodes such as $LiCoO_2$ and $LiFePO_4$ have specific capacities between 130 mAh/g and 170 mAh/g. Though the specific capacities of CuHCF and NiHCF are lower, their inexpensive synthesis, high rate capability, long cycle life and safety make them especially suitable for use in large scale stationary applications, such as energy storage related to the grid, for which weight and size are not as important as they are for portable electronics and vehicles. For this study, 60 mA/g is defined as 1C. Thus, 50 mA/g is equivalent to 0.83C, and 2500 mA/g to 41.7C.

Both CuHCF and NiHCF show complex behavior over a wide potential range during the cycling of Li^+ (Fig. 2b and 3b). In contrast, the potentials of both CuHCF and NiHCF during insertion and extraction of both Na^+ and K^+ followed smooth S-curves, indicative of solid solution reactions, consistent with previous observations on Prussian Blue and its analogs (Fig. 2c–2d and 3c–3d).[19,21–23,33] The same was true for NH_4^+ in CuHCF (Fig. 2e). The Li^+ insertion reaction occurred over a broader potential range than was found for Na^+

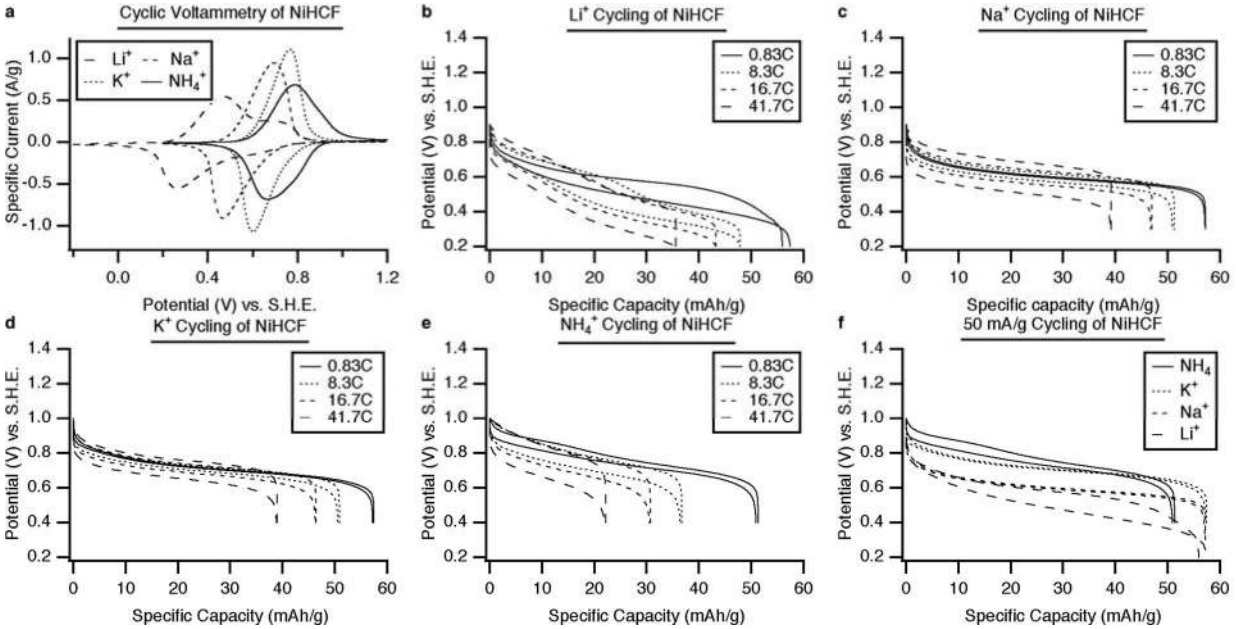

Figure 3. Electrochemical performance of NiHCF. Cyclic voltammetry of NiHCF with Li^+, Na^+, K^+ and NH_4^+ ions, and (b) through (e): The potential profiles of NiHCF during galvanostatic cycling of Li^+, Na^+, K^+, and NH_4^+, respectively, at several current densities. (f) The potential profiles of NiHCF during galvanostatic cycling of Li^+, Na^+, K^+, and NH_4^+, at 50 mA/g (0.83C). The potential profiles of NiHCF during Na^+ and K^+ cycling are adapted from Ref. 32.

and K^+ insertion. At the 0.83C rate, the potential range for full capacity in both CuHCF and NiHCF was 0.3 to 0.4 V for their reactions with Na^+, K^+ and NH_4^+, but the potential varied more widely, over a 0.7 V span during the insertion of Li^+ into CuHCF, over a 0.5 V span during Li^+ insertion into NiHCF. These results are consistent with a previous study of electrodeposited thin films of NiHCF, in which sharp reactions with Na^+ and K^+, but a broader reaction with Li^+, were observed.[21] In another study, electrodeposited films of Prussian Blue showed a much sharper reaction with K^+ than with NH_4^+, a result contradictory to that observed here.[33]

In addition, there was a slight indication of a shoulder at a charge state of about one third during cycling of Li^+ in CuHCF. This was also found in NiHCF, but only at higher current densities. This feature did not appear at the lower 0.83C rate in that case. A shoulder, and the presence of a second plateau, also appeared during the reaction of NH_4^+ ions with NiHCF. Finally, the reaction potentials of both CuHCF and NiHCF were found to increase for the heavier alkali ions, and the highest reaction potentials were observed during the cycling of NH_4^+ (Fig. 2e and 3e).

Both CuHCF and NiHCF displayed high rate capability, retaining most of their capacities at high current densities. This may be attributed to the porous, nanoparticulate electrode morphology, and to the rigid, open framework crystal structures of these materials. The high-rate capacity retention of CuHCF is greatest when it is cycled with K^+, for during this cycling it has 94.7% capacity retention at 8.3C, and 84% at 41.7C (Fig. 4a). Insertion of NH_4^+ and Li^+ into CuHCF also occurs readily at high rates, as it retains 75% and 65% of its discharge capacity during these respective reactions, at 41.7C. On the other hand, CuHCF showed poor rate capability during reaction with Na^+, retaining only 34% of its low rate capacity at 41.7C. During the reaction with both Na^+ and K^+, NiHCF retained 86% of its discharge capacity when cycled at 8.3C, and 66% at 2500 mA/g, a 41.7C rate (Fig. 4b). In contrast, the high rate behavior of NiHCF during the cycling of Li^+ and NH_4^+ was found to be less impressive, with only 58% and 39% of the slow rate discharge capacities retained at a 41.7C rate in those cases. These results compare favorably with the capacity retention of fast lithium-ion battery electrodes such as $LiFePO_4$, as well as with the sodium ion electrode material $Na_4Mn_9O_{18}$.[10,35,36]

Thus, both CuHCF and NiHCF showed high rate capability during the insertion of K^+ and NH_4^+, but behaved very differently when cycling Li^+ and Na^+. Lithium ions can easily be cycled in CuHCF at high rates, while Na^+ cannot; the opposite was found for NiHCF. The reason for the difference in the behavior of Li^+ and Na^+ these materials, whose lattice parameters differ by less than 1%, is not currently understood.

Experiments were also undertaken to evaluate the behavior of these materials during extended cycling at a 8.3C rate (500 mA/g) in Li^+, Na^+, K^+, and NH_4^+ electrolytes. CuHCF showed excellent durability during long cycling at that rate in electrolytes containing K^+ ions, retaining 99% of its initial capacity after 500 cycles (Fig. 4c). The capacity retention of CuHCF during its reaction with the other ionic species was found to be lower, retaining 91%, 77%, and 35% of the initial capacity after 500 cycles in NH_4^+, Na^+, and Li^+, respectively.

NiHCF showed no measurable capacity loss during 500 cycles in electrolytes containing either Na^+ or K^+ (Fig. 4d). After an initial capacity loss of about 10% during the first 100 cycles, the capacity of NiHCF remained stable during the cycling of NH_4^+, retaining 88% of its initial capacity after 500 cycles. However, NiHCF showed severe capacity loss during cycling with Li^+, as did CuHCF. It was observed that the electrolyte turned yellow, indicating that species in the electrode had dissolved into the electrolyte. It remains unclear, however, why the insertion of Na^+ into CuHCF results in substantial capacity loss, but NiHCF shows perfect stability when cycled under the same conditions.

As has been demonstrated above, the materials investigated in this work had much better cycle life with some insertion species than with others. One explanation for these differences is that the solubility of CuHCF and NiHCF during cycling may vary between electrolytes. The counter electrodes used in these experiments contained large masses of the same hexacyanoferrate active materials as the working electrodes. This ensured that the counter electrodes acted as reversible ion sinks with only small changes in their potentials, and helped avoid spurious side reactions, such as electrolyte decomposition. However, the presence of large masses of CuHCF and NiHCF in the counter electrodes might have masked the effects of trace solubility of these materials in aqueous electrolytes. Visual observation of a color change, which is assumed to be due to the presence of dissolved $Fe(CN)_6^{-3}$,

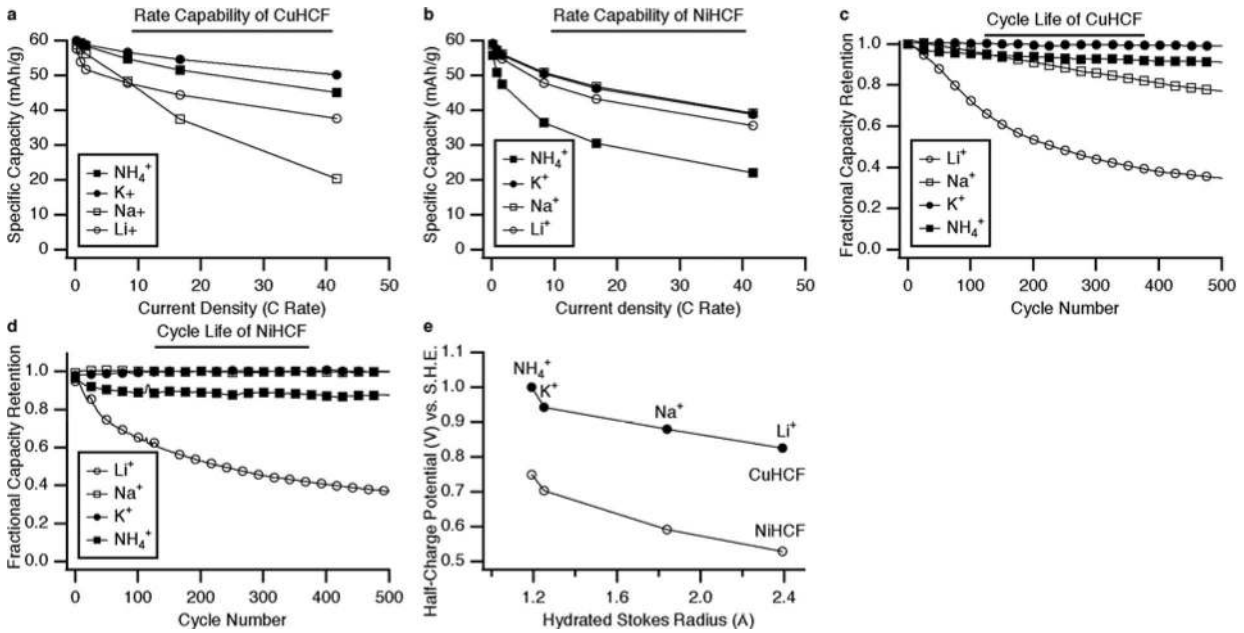

Figure 4. Rate capability, cycle life, and effect of insertion ion size on CuHCF and NiHCF. (a) and (b) The capacity retention of CuHCF and NiHCF at various densities. (c) and (d) The cycle life of CuHCF and NiHCF during cycling of Li^+, Na^+, K^+, and NH_4^+, and (e) The reaction potentials CuHCF and NiHCF as functions of the Stokes radius of the insertion ion. The capacity retention of NiHCF during Na^+ and K^+ cycling is adapted from Ref. 32.

during the insertion of Li^+ into both CuHCF and NiHCF, indicated that the observed capacity losses in those cases were caused at least in part by dissolution of the active material. The smaller capacity losses observed during the cycling of NH_4^+ for both materials, and during the cycling of Na^+ in CuHCF might be attributed to slower dissolution in those cases. Future study of the solubility of CuHCF, NiHCF, and other Prussian Blue analogs in a variety of aqueous electrolytes will establish the conditions under which they may be operated with long cycle life in full cells that do not contain excess ferricyanide in the counter electrode.

One possible interpretation of this behavior involves the size of the inserted species, often expressed in terms of the Stokes radius, which is a parameter experimentally determined by experiments in aqueous systems. The higher the charge to radius ratio of an ion, the more strongly water molecules will coordinate to it, so a smaller effective ionic radius results in a larger Stokes radius in aqueous solutions. A study of electrodeposited Prussian Blue thin films for electrochromic devices noted that only insertion species with Stokes radii smaller that the radii of the channels between the A sites in the electrode's crystal structure could be readily cycled.[20] This result is consistent with the general approach to the movement of ions through the windows in interstitial space in solids. However, demonstration of Na^+ cycling in NiHCF thin films,[21,22] further bolstered by the results presented here, conflict with this interpretation of the maximum allowable size for insertion ions in the Prussian Blue structure: the Stokes radius of aqueous Na^+ and Li^+ are generally considered to be about 1.8 Å and 2.4 Å, respectively,[37] while the radii of the channels connecting the A sites are assumed to be about 1.6 Å.[20] The reaction potentials in both CuHCF and NiHCF measured in this work are higher for the heavier and larger inserted ions. That is, they decrease with an increase in the Stokes radius of the insertion ion (Fig. 4e), as found in earlier results on Prussian Blue and NiHCF.[21,33]

The differences in the kinetic properties of different hydrated ions in the Prussian Blue structure materials may not be just a matter of the apparent size of these ions. It is also possible that motion of these ionic groups through the windows in the crystal structure involve interchange of nearby water molecules, and the effective rotation of the hydration sheaths about the inserted ions. This phenomenon is related to the unusually fast transport of lithium ions found in solid lithium sulfates, which has been interpreted in terms of the rotation of the surrounding sulfate groups.[38–40] This rotation-assisted ionic transport has been called a "cogwheel", or "paddlewheel" mechanism.

Both CuHCF and NiHCF, as well as other materials in the Prussian Blue hexacyanoferrate family, are mixed conductors that exhibit both thermodynamic and electronic properties similar to those of materials in the oxide bronze families, such as H_xWO_3, another well-known electrochromic material.[41] The variation of the electrical potential during charge and discharge is related to the change in the chemical potential of the neutral guest species as a function of its concentration.

The chemical potential of a mixed conductor can be formally divided into two components, one relating to the ions, and the other to the electrons.[41,42] The first is the influence of the change in the concentration of the ionic guest species on the enthalpy and configurational entropy of the guest ions. It is the contribution due to the configurational entropy of the ions that leads to the typical S-shape in the equilibrium discharge curves of such materials. The second component of the chemical potential of a mixed conductor is the influence of the change in the electron composition in the host material, i.e. the composition dependence of the Fermi level of the degenerate electron gas.

In the free-electron model, which has been found to be applicable to these types of materials, the Fermi level, related to the negative value of the electrochemical potential, is proportional to the two-thirds power of the electron concentration, and thus the guest species concentration, divided by the effective mass of the electrons. Changes in this latter parameter, the effective electronic mass, thus influence the slope of the potential profile. It is expected that the effective electronic mass would depend upon the identity of the inserted ion. These features of the data can be seen in Figs. 2 and 3, where heavier and larger alkali ions generally have higher reaction potential curves in both CuHCF and NiHCF. Changes in the slope of reaction curves of the different materials measured under the same conditions are especially visible in the data in Fig. 2f and 3f.

Conclusions

Inexpensive, scalable, low temperature methods were used to prepare large quantities of nanoparticulate CuHCF and NiHCF. X-ray

diffraction found that these materials are highly crystalline and phase pure. Transmission electron microscopy showed that the resulting CuHCF and NiHCF are composed of 20–50 nm grains, which form large, porous agglomerations. These materials were found to be electrochemically active in aqueous electrolytes containing Li^+, Na^+, K^+, and NH_4^+. Rapid kinetics and long cycle life were observed for the reaction of K^+ with CuHCF, and for the reactions of Na^+ and K^+ with NiHCF. Both electrode materials also showed electrochemical activity in the presence of Li^+ and NH_4^+, though with more limited rate capability and cycle life. The decay in the performance of both CuHCF and NiHCF when cycled in electrolytes containing Li^+ may be readily explained by their dissolution. The discrepancy between the consistent capacity loss of CuHCF with Na+, and the completely stable cycling of NiHCF with Na^+, under the same conditions cannot yet be explained. Though the reaction potentials and their slopes in both CuHCF and NiHCF correlate with the size of the inserted ions, additional study must occur to elucidate the conditions that lead to capacity loss.

Acknowledgments

The authors acknowledge partial support from the King Abdullah University of Science and Technology (KAUST) Investigator Award (No. KUS-l1-001-12). A portion of this work was supported by the Department of Energy, Office of Basic Energy Sciences, Division of Materials Sciences and Engineering under contract DE-AC02-76SF00515 through the SLAC National Accelerator Laboratory LDRD project.

References

1. Z. Yang, J. Zhang, M. C. W. Kintner-Meyer, X. Lu, D. Choi, J. P. Lemmon, and J. Liu, *Chem. Rev.*, **111**, 3577 (2011).
2. G. L. Soloveichik, in *Annu. Rev. Chem. Biomol. Eng.*, **2**, J. Prausnitz, Editor, p. 503, Annu. Rev. Inc., Palo Alto, CA (2011).
3. D. Howell, *Annu. Prog. Report 2008 Energy Storage Research and Development.* DOE Energy Efficiency and Renewable Energy (2009).
4. K. H. LaCommare and J. H. Eto, *Understanding the Cost of Power Interruptions to U.S. Electricity Consumers.* DOE Environmental Energy Technologies Division. LBNL-5518 (2004).
5. Y. V. Makarov, C. Loutan, J. Ma, and P. de Mello, *IEEE Trans. Power Systems*, **24**, 1039 (2009).
6. J. P. Barton and D. G. Infield, *IEEE Trans. Energy Conversion.* **19**, 441 (2004).
7. R. Ruffo, C. Wessells, R. A. Huggins, and Y. Cui, *Electrochem. Comm.*, **11**, 247 (2009).
8. J.-Y. Luo, W.-J. Cui, P. He, and Y.-Y. Xia, *Nature Chem.*, **2**, 760 (2010).
9. C. Wessells, R. A. Huggins, and Y. Cui, *J. Power Sources*, **195**, 2884 (2011).
10. J. F. Whitacre, A. Tevar, and S. Sharma, *Electrochem. Comm.*, **12**, 463 (2010).
11. N. L. Rosi, J. Eckert, M. Eddaoudi, D. T. Vodak, J. Kim, M. O'Keeffe, and O. M. Yaghi, *Science*, **300**, 1129 (2003).
12. M. Dinca, S. W. Han, Y. Liu, A. Dailly, C. M. Brown, and J. R. Long, *J. Am. Chem. Soc.*, **128**, 16876 (2006).
13. G. Férey, F. Millange, M. Morcrette, C. Serre, M.-L. Doublet, J.-M. Grenéche, and J.-M. Tarascon, *Angew. Chem. Int. Ed.*, **46**, 3259 (2007).
14. M. B. Robin, and P. Day, *Adv. Inorg. Chem.*, **10**, 247 (1968).
15. A. Ludi and H. U. Güdel, in *Structure and Bonding*., Vol. 14, J. D. Dunitz, P. Hemmerich, J. A. ibers, C. K. Jorgensen, J. B. Neilands, R. S. Nyholm, D. Reinen, and R. J. P. Williams, Editors, p. 1, Springer, New York (1973).
16. H. J. Buser, D. Schwarzenbach, W. Petter, and A. Ludi, *Inorg. Chem.*, **16**, 2704 (1977).
17. F. Herren, P. Fischer, A. Ludi, and W. Halg, *Inorg. Chem.* **19**, 956 (1980).
18. K. Itaya, I. Uchida, and V. D. Neff, *Acc. Chem. Res.*, **19**, 162 (1986).
19. V. D. Neff, *J. Electrochem. Soc.*, **125**, 886 (1978).
20. K. Itaya, T. Ataka, and S. Toshima, *J. Am. Chem. Soc.*, **104**, 4767 (1982).
21. A. B. Bocarsly and S. Sinha, *J. Electroanal. Chem.*, **140**, 167 (1982).
22. S. Sinha, B. D. Humphrey, and A. B. Bocarsly, *Inorg. Chem.*, **23**, 203 (1984).
23. L. M. Siperko and T. Kuwana, *J. Electrochem. Soc.*, **130**, 396 (1983).
24. T. Oi, in *Ann. Rev. Mater. Sci.*, Vol. 16, R. A. Huggins, Editor, p. 185, Ann. Rev., Inc., Palo Alto, CA (1986).
25. D. E. Stilwell, K. H. Park, and M. H. Miles, *J. Appl. Electrochem.*, **22**, 325 (1992).
26. V. D. Neff, *J. Electrochem. Soc.*, **132**, 1382 (1985).
27. E. W. Grabner and S. Kalwellis-Mohn, *J. Appl. Electrochem.*, **17**, 653 (1986).
28. K. Honda and H. Hayashi, *J. Electrochem. Soc.*, **134**, 1330 (1987).
29. M. Kaneko and T. Okada, *J. Electroanal. Chem.*, **255**, 45 (1988).
30. S. Kalwellis-Mohn and E. W. Grabner, *Electrochemica Acta*, **34**, 1265 (1989).
31. C. D. Wessells, R. A. Huggins, and Y. Cui, *Nature Comm.*, In press, 2011.
32. C. D. Wessells, S. V. Peddada, R. A. Huggins, and Y. Cui, *Nano Letters*, In press, 2011.
33. J. W. McCargar and V. D. Neff, *J. Phys. Chem.*, **92**, 3598 (1988).
34. S. S. Kaye and J. R. Long *J. Am. Chem. Soc.*, **127**, 6506 (2005).
35. B. Kang and G. Ceder, *Nature*, **458**, 190 (2009).
36. G. Ceder and B. Kang, *J. Power Sources*, **194**, 1024 (2009).
37. P. C. F. Pau, J. O. Berg, and W. G. McMillian, *J. Phys. Chem.*, **94**, 2671 (1990).
38. A. Kvist and A. Bengtzelius, in *Fast Ionic Transport in Solids*, W. van Gool, Editor, p. 193, North Holland Pub. Co., Amsterdam (1973).
39. A. Lunden and J. O. Thomas, in *High Conductivity Solid Ionic Conductors*, T. Takahashi, Editor, p. 45, World Scientific, Singapore (1989).
40. A. Lunden, in *Fast Ion Transport in Solids*, B. Scrosati, A. Magistris, C. M. Mari, and G. Mariotto, Editors, p. 181, Kluwer Academic Publishers, Dordrecht (1992).
41. I. D. Raistrick, A. J. Mark, and R. A. Huggins, *Solid State Ionics*, **5**, 351 (1981)
42. R. A. Huggins, *Advanced Batteries: Materials Science Aspects*, p. 116–119, Springer, New York (2010).